MECHANICAL BEHAVIOUR OF VACUUM CHAMBERS AND BEAM SCREENS UNDER QUENCH CONDITIONS IN DIPOLE AND QUADRUPOLE FIELDS

C. Rathjen, CERN, Geneva, Switzerland

Abstract

A method based on analytical formulas is described to calculate bending moments, stresses, and deformations of vacuum chambers and beam screens in dipole and in quadrupole fields during a magnet quench. Solutions are given for circular and racetrack shaped structures. Without the need of time consuming calculations the solutions enable a quick design and verification of vacuum chambers and beam screens.

1 INTRODUCTION

A time variant magnetic field induces eddy currents in any conductive structure inside the field. In combination with the magnetic field, Lorentz forces on the structure are generated. In particular vacuum chambers and beam screens of colliders, like the LHC, are subjected to high forces because of their high conductivity necessary for low machine impedance and the strong magnetic fields. Highest mechanical loads are generated during a quench (resistive transition of a super conducting magnet).

This note treats eddy currents in dipole and quadrupole fields as shown exemplarily in Fig. 1 and 2 for the case of a LHC beam screen. Besides circular tubes, racetrack shaped structures are investigated which where developed to integrate cooling tubes inside vacuum chambers.

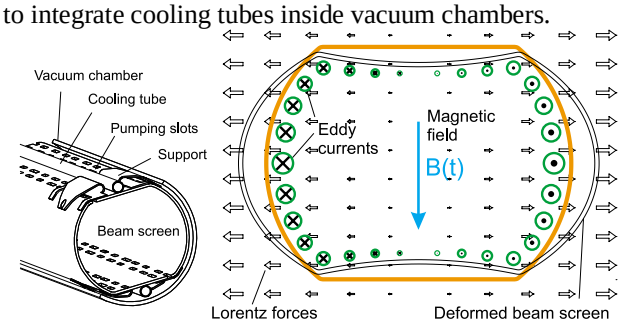

Figure 1: Eddy currents, Lorentz forces and deformations of a beam screen in a dipole field during quench.

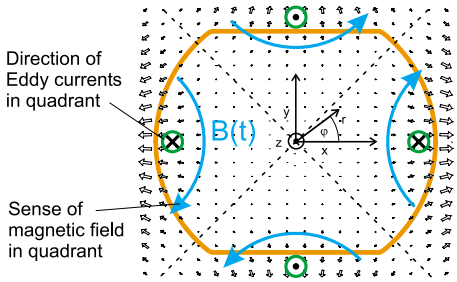

Figure 2: Beam screen in a quadrupole field during quench with superposed field of Lorentz forces.

Assuming quasi static conditions, the integration of Faraday's law $\nabla\times\mathbf{E}=-\partial\mathbf{B}/\partial t$ gives the electrical field vector **E** [1]. For dipole fields $E_z=-\partial B/\partial t\, x$, where B is the flux density of the magnetic field. For a quadrupole field $E_z= r^2/2\ \partial G/\partial t \cos(2\varphi)$, where G is the field gradient of the magnetic field defined by $B_x=G\,y$ and $B_y=G\,x$. The two-dimensional modelling in Fig. 1 and 2 is justified since **E** has only a z-component and the shape of the structures is long and prismatic.

E is the electromotive force driving the eddy currents $\boldsymbol{j}$ which are calculated using Ohms law and the resistivity ρ of the structure. Eddy currents form closed loops inside the structure, either at the ends or in regions where the magnetic field vanishes. Volumetric Lorenz forces $\boldsymbol{f}$ on the structure are calculated using $\boldsymbol{f}=\boldsymbol{j}\times\mathbf{B}$. For dipole fields

$$f_x = -\frac{x\,B}{\rho}\frac{\partial B}{\partial t} \tag{1}$$

and for quadrupole fields

$$f_x = -\frac{1}{2}\frac{r^3\cos(\varphi)\cos(2\varphi)\,G}{\rho}\frac{\partial G}{\partial t}, \tag{2}$$

$$f_y = \frac{1}{2}\frac{r^3\sin(\varphi)\cos(2\varphi)\,G}{\rho}\frac{\partial G}{\partial t}. \tag{3}$$

2 MECHANICAL MODEL

2.1 Assumptions and limitations

Only the case where the wall thickness is small compared to the size of the structure is covered. This can be described with Lorentz forces concentrated on the neutral fibre of the structure and deformation only due to bending. The resistivity ρ is assumed to be constant.

2.2 Derivation of analytical solutions

Due to symmetry it is sufficient to treat a quarter of the structure. Fig. 3 shows the model and defines the mechanical quantities used in the following. With the boundary condition of no rotation at the free end (ψ=0) deformations are according to the force fields in Fig. 1 and 2. The displacement w_v is identical to the deformation along vertical axis of symmetry. The internal force Q is equal to the integral of the vertical Lorentz forces (d is the thickness of the conducting layer; Q=0 in dipole fields):

$$Q = \int_0^{\Phi} d\ f_y(\varphi)\, r\ d\varphi + \int_0^{x(\Phi)} d\ f_y(x)\ dx. \tag{4}$$

The principle of virtual work

$$\overline{M}\psi \vee \overline{F}_h w_h \vee \overline{F}_v w_v = W = \int \frac{M(s)\overline{M}(s)}{EI(s)} ds \tag{5}$$

is used to derive analytical solutions. EI is the bending stiffness of the structure. $M(s)$ is the internal bending moment at a certain location s along the structure due to the Lorentz forces and the unknown internal moment M_b. $\overline{M}(s)$ is the corresponding bending moment for the virtual moments and forces according to Fig. 3 bottom. The

unknown M_b is calculated using $\overline{M}_\psi = 0 = W$. This yields $M(s)$ necessary to calculate the deformations w_h and w_v using Eq.(5). Note that the integration along s has to be done in one direction; thus in the flat part $ds = -dx$ and

$$W = \int_0^{\Phi} \frac{M(\varphi)\overline{M}(\varphi)}{EI(\varphi)} r\, d\varphi - \int_{x(\Phi)}^{0} \frac{M(x)\overline{M}(x)}{EI(x)}\, dx\,. \qquad (6)$$

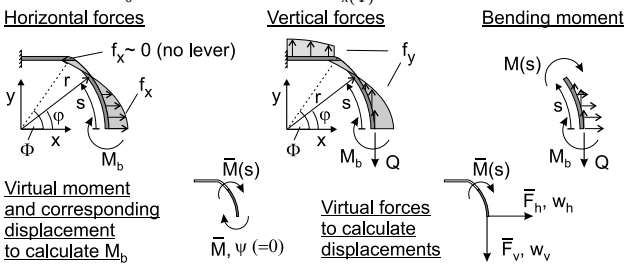

Figure 3: Mechanical model for horizontal and vertical Lorentz forces (shown for quadrupole fields) and virtual quantities to calculate the unknowns M_b, w_h and w_v.

3 RESULTS

The results given in the following are for structures of constant wall thickness h where a portion d of the wall is conductive (e.g. a copper layer). Results are given in normalised diagrams Fig. 4-7 where the angle of the corner Φ varies with aspect ratio. The diagrams include all necessary information for a quick calculation of structures of all different aspect ratios.

The equations for the bending moment and the displacement are not shown here since they are very long. The diagrams given have a sufficiently high resolution to allow precise calculations. However, if equations are desired it is recommended to solve the integrals in Eq. (6) with the aid of a computer algebra program. To verify the implementation of Eq. (6) and to reproduce Fig. 5 with a higher resolution, the equation for the bending moment in the curved part of a structure is given below for the case of a dipole field:

$$\frac{M(\varphi)}{M_0} = \frac{4\left(\Phi + \cos(\Phi)\right)\cos(\varphi)^2 - 2\Phi - \sin(2\Phi) - 4\cos^3(\Phi)}{8\left(\Phi + \cos(\Phi)\right)}\,.$$

Displacements are given only along the vertical and horizontal axes of symmetry where they are maximal due to the shape of the force fields and the symmetry of the structure.

Stresses: For a homogeneous wall, where $EI = Eh^3/12$, the stresses can be calculated from the bending moment M with the aid of $\sigma = 6M/h^2$ (otherwise theory of composite materials has to be used).

4 DISCUSSION

Field properties, material and the size of the structure scale the solutions; the angle Φ determines the shape.

Fig. 4: Since $\partial B/\partial t$ is negative during a quench, the structure expands horizontally and contracts vertically. Horizontal and vertical deformations are roughly the same. To reduce deformations it is more advantageous to increase the wall thickness rather than to reduce Φ (i.e. the vertical aperture).

Fig. 5: Apart form circular tubes the bending moment (i.e. stresses) is maximal in the horizontal axis of symmetry. Stress concentration in the corner can result in even higher stresses.

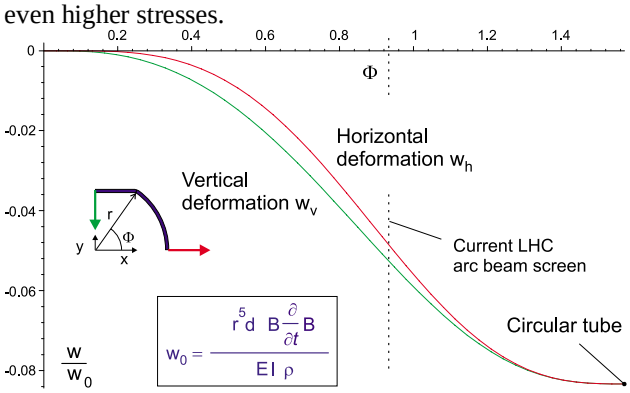

Figure 4: Normalised horizontal deformation in dipole field for structures of different aspect ratios.

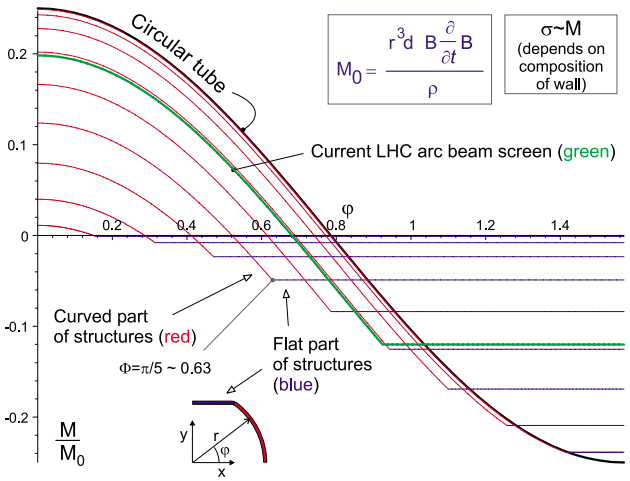

Figure 5: Normalised bending moment in dipole field for structures of different aspect ratios.

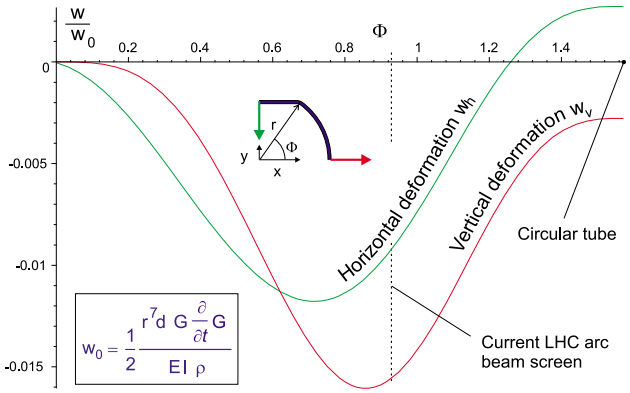

Figure 6: Normalised deformations in quadrupole field for structures of different aspect ratios.

Fig. 6: As in dipole fields, the structure expands horizontally and contracts vertically during a quench. Vertical expansion (e.g. possible contact of cooling tube to vacuum chamber in Fig. 1) can only occur if structures are almost circular. The maximum horizontal deformation at Φ=0.86 is 5.8 times higher than the one for the circular tube; in the vertical direction the factor is –4.2 at Φ=0.72.

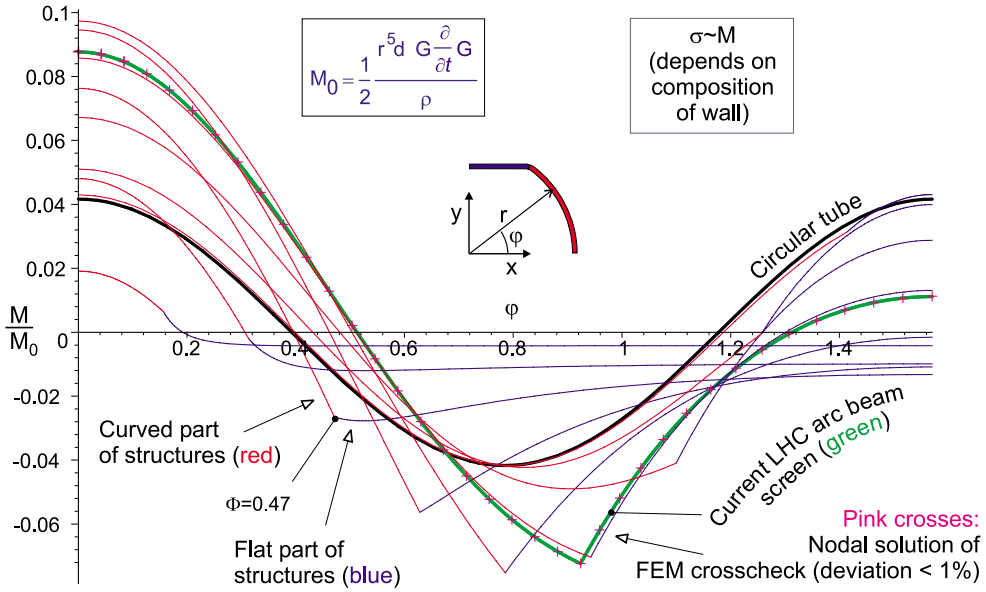

Figure 7: Normalised bending moment in quadrupole field for structures of different aspect ratios.

Fig. 7: Stresses are always highest in the horizontal plane (φ=0). Excluding very flat beam screens (Φ<0.325) it can be concluded that the introduction of the flat parts aggravates bending moments (i.e. stresses). In the worst case (Φ=0.73), stresses are a factor of 2.4 higher than in a circular tube.

5 APPLICATION

The results given above are conservative since the assumption of a constant resistivity in Eq. 1-3 is a worst-case approach. Any heat-up due to eddy currents will increase the resistivity and therefore reduce Lorentz forces. The same is valid in the case of magneto resistance in quadrupole fields (proportional to the radius *r* in Fig. 2): In a racetrack type structure the resistance in the flat parts will be lower than in the curved parts. This causes higher Lorentz forces at a certain angular position φ in Fig. 2. Higher forces in the flat part move the bending moment towards the solution for a circular tube (Fig. 7), which has lower maximal stresses (for aspect ratios of practical interest).

For thin-shelled structures, as the LHC arc beam screen, with a highly conductive copper layer (50 µm) at the inside, the results agree well with FEM calculations with forces not concentrated on the neutral fibre of the structure. Also sophisticated calculations taking into account heating effects and thermal conduction do not differ more than 10% for LHC arc beam screens in dipole fields. More critical is the knowledge of the real material properties where the biggest errors occur. Presently 30% higher displacements than measured [2] are obtained with the results above. Limitations are the inhomogeneous resistivity and thickness of the copper layer.

Comparison of LHC arc beam screens (r =23.75 mm, Φ=0.924, $G\partial G/\partial t$=2.3×10^5 T^{2}m^{-2}s^{-1}, $B\partial B/\partial t$=200 T^{2}s^{-1}) yields to 7 times higher bending moments (i.e. stresses) and 9 times higher horizontal deformations in LHC dipole magnets; quadrupole magnets are therefore not critical. Keeping $(G\partial G/\partial t)/(B\partial B/\partial t)$ constant, bending moments are equal to each other if the radius r is increased by a factor of 2.6 (see proportionalities to r in Fig. 5 and 7: $\propto r^3$ for dipole fields and $\propto r^5$ for quadrupole fields). Structures can therefore be more critical in quadrupole magnets than in dipole magnets when the dimensions increase.

If the structure has holes (e.g. pumping slots in Fig. 1) stress concentration occurs. If the energy expressed by Eq. (6) does not vary significantly, stress increase can be estimated according to the following example: In the case of a beam screen with rounded slots and a slot coverage of 50%, stresses are 1.5 times higher due to the shape of slots and 2 times higher due to the missing material.

6 CONCLUSIONS

The presented results, based on analytical formulas, give insight how the aspect ratio of a racetrack shaped structure influences its mechanical behaviour compared to a circular structure. The results enable a quick, conservative estimation of stresses and deformations of beam screens and vacuum chambers in varying dipole and quadrupole fields. In the future they will be applied for the long straight section of the LHC where many chambers and screens have to be investigated. Other applications are fast ramping magnets, as foreseen for future projects at the GSI. For different geometries, analytical solutions can be derived as presented.

7 REFERENCES

[1] H.A. Haus et al., "Electromagnetic fields and energy", Prentice-Hall International, Inc. 1990.

[2] C. Rathjen et al., "Currents in, Forces on and Deformations/Displacements of the LHC Beam Screen expected during a Magnet Quench", TOAB005, Proc. of the 2001 Particle Accelerator Conference, Chicago.